Low-energy O^+ or SiO^+ ion beam induced deposition of silicon oxide using hexamethyldisiloxane

Satoru Yoshimura[1*], Takae Takeuchi[1], and Masato Kiuchi[1,2]

[1]*Division of Materials and Manufacturing Science, Graduate School of Engineering, Osaka University, Suita, Osaka 565-0871, Japan.*

[2]*Cerast Laboratory, Setagaya, Tokyo 154-0011, Japan*

*corresponding author

E-mail: yosimura@ppl.eng.osaka-u.ac.jp (SY).

Abstract

We attempted to form silicon oxide films by spraying hexamethyldisiloxane (HMDSO) to a substrate together with low-energy O^+ ion beam injections. The energy of O^+ ions was 100 eV. The substrate temperature was set at room temperature. After the trial, we found a film deposited on the substrate. X-ray photoelectron spectroscopy (XPS) measurements of the film showed that the film was silicon dioxide. The XPS spectra of the film also showed that the film contained almost no carbon atoms. For comparison, 100 eV SiO^+ ion beams were injected into a substrate at room temperature in conjunction with HMDSO. XPS results of the deposited film showed that the film was silicon oxide and the atomic concentration ratio of oxygen to silicon was 1.35. In this case, however, a relatively large amount of carbon atoms (12 atomic%) was included in the film. In conclusion, we confirmed that the 100 eV O^+ ion beam induced deposition using HMDSO is useful for the silicon dioxide film formation.

Keywords:

silicon oxide;

hexamethyldisiloxane;

molecular ion beam deposition;

ion beam induced chemical vapor deposition

1. Introduction

The ion beam technique is available for film formations of various materials [1, 2]. There are several film depositing methods using the ion beam technique.

We are now studying two film deposition methods based on the ion beam technique, i.e., the molecular ion beam deposition method [3] and the ion beam induced chemical vapor deposition (IBICVD) method [4-6]. In the molecular ion beam deposition method, a source material is dissociated in an ion source and molecular ions are mass-selected from various fragment ions produced by the decomposition of the source material. Then, the molecular ions are irradiated to a substrate and thus, a film is deposited on the substrate. On the other hand, in the IBICVD method, a source material and ion beams such as O^+ and Ar^+ are simultaneously injected to a substrate. Recently, we also conducted an experiment integrating the molecular ion beam deposition method with the IBICVD method [7].

Meanwhile, silicon oxide films are useful as an insulating film in semiconductor technologies. Silicon oxide films can be formed by chemical vapor deposition (CVD)

using silane [8] or tetraethyl orthosilicate (TEOS) [9].

Hexamethyldisiloxane (HMDSO, $(CH_3)_3SiOSi(CH_3)_3$)) has also been used as a source material for the formation of silicon oxide films. Many studies in which silicon oxide film formations were performed using HMDSO have been published [10-20]. However, only a few papers in which HMDSO was used as a source material for ion beam deposition experiments are available. Recently, Yoshimura et al. succeeded in depositing silicon oxide films by the molecular ion beam method [21]. In their experiments, SiO^+ ion beam produced by the decomposition of HMDSO was injected to a substrate and then, a silicon oxide film was formed on the substrate. On the other hand, Matsutani et al. performed an IBICVD experiment using HMDSO [22]. They irradiated a substrate by 150 eV O^+ ion beams while spraying HMDSO on the substrate, confirming that a silicon oxide film was formed on the substrate. However, in those previous experiments, the optimal injecting ion energy level has not been investigated yet. In addition, no experiments where HMDSO was sprayed on a substrate and SiO^+ ions were simultaneously injected to the substrate, have been conducted so far.

In most cases, silicon oxide films deposited by the methods such as CVD [8-20] were

uniformly formed on the substrates. On the other hand, films deposited by the ion beam technique were formed at the location where the ion beam contacted the substrate. In fact, we confirmed that a film could be deposited on a limited local site of the substrate with the molecular ion beam deposition method [23] or with the IBICVD method [24].

In this study, we conducted an experiment in which HMDSO was sprayed onto a substrate and the substrate was also simultaneously irradiated with O^+ or SiO^+ ions. The mass and the energy of the injecting ions were firstly measured. The ion energy of O^+ or SiO^+ ions was set at 50, 100, or 200 eV. Trials for 50, 100, and 200 eV were performed and the resulting film thicknesses were evaluated. We found that the ion energy at which the obtained film thickness was maximal was 100 eV for both O^+ and SiO^+ cases. After the film deposition by 100 eV O^+ or SiO^+ ion beam injections to a substrate in conjunction with HMDSO, the obtained films were analyzed by X-ray photoelectron spectroscopy (XPS) and Fourier transform infrared (FTIR) spectroscopy.

2. Materials and Method

The experimental trials were carried out using an ion beam machine (ULVAC) [25] with

a Freeman-type ion source. This machine was originally prepared for the investigation of the interaction between ion beams and various materials (e.g., sputtering yield of various materials by ion beam injections) [26, 27]. Since the machine was not designed for film formation experiments, the ion beam intensity was relatively weak when compared with the ion beam machines, commonly used for film depositions. In this study, we produced low-energy O^+ and SiO^+ ion beams using the ion beam machine.

The source gas for the O^+ ion beam was CO_2. In the O^+ ion beam production, the operational parameters for the ion source were as follows: The source gas flow rate, the current being applied to a tungsten filament, the magnetic field applied in an arc chamber, the arc voltage (the bias voltage between the arc chamber and the tungsten filament), and the arc current were 1 sccm, 130 A,10 mT, 75 V, and 0.5 A, respectively. The procedures for the ion beam production were as follows. Firstly, CO_2 was dissociated in the ion source. The resulting dominant ions were found to be C^+, O^+, and CO^+. All these ions were extracted by applying a high voltage (-15 kV), and only O^+ ions were selected by a mass-selector. The mass-selected O^+ ion beam was guided to a process chamber and was slowed down by a decelerator to obtain a low-energy O^+ ion beam.

On the other hand, the source material for the SiO^+ ion beam production was HMDSO. HMDSO was bubbled with argon gas and a mixed gas of HMDSO and argon was introduced into the ion source. HMDSO was dissociated in the ion source. Only SiO^+ ions were mass-selected from various fragment ions produced by the decomposition of HMDSO. The SiO^+ ion beam was guided to the process chamber and was slowed down to obtain a low-energy SiO^+ ion beam. The intensity of SiO^+ ion beams obtained under the operational parameters mentioned above was found to be too small. Therefore, in the SiO^+ ion beam experiment, the arc current was increased to be 1.8 A.

A schematic drawing of the process chamber of the ion beam machine is shown in Fig. 1. The low-energy O^+ or SiO^+ ion beam was injected to a substrate at normal incidence. The vacuum degree in the chamber was 1×10^{-6} Pa. On the process chamber, an ion mass-energy analyzer (balzers, PPM-421) was installed, as shown in Fig. 1. We used a gold-coated quartz crystal microbalance (QCM) substrate (ULVAC, CRTS-0) as a target of ion beam injections. The details of the QCM system were presented in our earlier paper [28]. The thickness of the film deposited on the QCM substrate can be evaluated using a QCM controller (ULVAC, CRTM-9000). The QCM substrate was used at room temperature. During the ion beam injections, HMDSO was also simultaneously sprayed

onto the substrate. HMDSO vapor was introduced directly to a mass flow controller and the flow rate of HMDSO was set at 0.7 sccm. The HMDSO pressure was 1×10^{-3} Pa in the process chamber. After the experimental trials, the deposited films were analyzed by XPS (ULVAC-PHI, ESCA-3057).

3. Results and discussion

Firstly, the mass spectra of ion beams were measured by the mass-energy analyzer. Fig. 2(a) shows the mass spectrum of an ion beam produced by the decomposition of CO_2. In Fig. 2(a), the mass peak is located at 16 u, showing that the ion beam was composed of O^+ ions. Fig. 2(b) shows the mass spectrum of an ion beam produced using HMDSO. The mass peak is at 44 u in Fig. 2(b), showing that this is SiO^+ ion beam. The beam current density was about 1 μA / cm^2 for the O^+ ion beam and about 0.1 μA / cm^2 for the SiO^+ ion beam.

Then, the energy spectra of ion beams were also obtained by the mass-energy analyzer. Figs. 3(a), 3(b), and 3(c) show the actual energy distributions of O^+ ions when the ion energy was set at (a) 50, (b) 100, and (c) 200 eV, respectively. Figs. 3(a)-3(c) show that the peak energies of the energy distributions approximately coincide with the set values.

Full width at half maximum of each energy distribution is about 15 eV in Figs. 3(a)-3(c). On the other hand, Figs. 4(a), 4(b), and 4(c) show the ion energy spectra of the SiO^+ ion beams in (a) 50, (b) 100, and (c) 200 eV cases, respectively. Full width at half maximum of each energy distribution is about 3 eV in Figs. 4(a)-4(c). The energy spectra of SiO^+ ions were different from those of O^+ ions because the operational parameters in the case of SiO^+ ion beam production were slightly different from those in the O^+ ion beam case. The peak energies were located at (a) 56, (b) 105, and (c) 205 eV in Figs. 4(a)-4(c). The actual SiO^+ ion energies were shifted from their nominal values because of kinetic energies reflecting the plasma potential in the ion source [29].

Prior to the film deposition trials, we injected 50 or 100 eV O^+ ion beams to a QCM substrate without supplying HMDSO, and found that no film was formed on the substrate. Trials in which HMDSO was sprayed to a QCM substrate without O^+ or SiO^+ ion beams also yielded no film formation.

Firstly, O^+ ion beams were injected to a QCM substrate while HMDSO was simultaneously sprayed to the substrate. Three trials in which the peak O^+ energy was 50, 100, or 200 eV were carried out. The duration of each trial was 60 min. After each trial, a

film was found formed on the substrate. The film thicknesses were measured by the QCM controller, and the results are presented in Fig. 5. Fig. 5 shows that the thickness of the film obtained in the 100 eV case was thicker than those in the 50 and 200 eV cases.

Secondly, a QCM substrate was injected by SiO^+ ion beams of 50, 100, or 200 eV while HMDSO was sprayed to the substrate. The duration of each trial was 60 min. The film thicknesses are presented by closed circles in Fig. 6. We found that the thickness in the 100 eV case was thicker than those in the 50 and 200 eV cases.

For comparison, a QCM substrate was injected by SiO^+ ion beams without supplying HMDSO to the substrate. Three trials in which the SiO^+ energy was 50, 100, or 200 eV were carried out. The duration of each trial was 60 min. The film thicknesses were measured by the QCM controller, and the results are presented by closed triangles in Fig. 6.

The difference between circles and triangles in Fig. 6 represents the effect of spraying HMDSO during the injection of SiO^+ ions. Fig. 6 shows that in the cases of 50 and 200 eV, the film thickness increased only slightly even when HMDSO was sprayed onto the substrate. On the other hand, in the case of 100 eV, the film thickness was significantly

increased by spraying HMDSO together with the SiO^+ ion injection.

In the experimental trials in Figs. 5 and 6, the duration of each trial was 60 min. Then, we elongated this duration for the increase of film thickness. Firstly, O^+ ion beams were injected to a QCM substrate while HMDSO was simultaneously sprayed to the substrate. The duration was 350 min. The injection ion energy was set at 100 eV because Fig. 5 demonstrated that the deposition rate in the 100 eV case was significantly larger than those in 50 and 200 eV cases. After the trial, we found that a film was formed on the QCM substrate. The QCM controller showed that the film thickness was 29 nm. Hereafter, we refer to this film as sample (a).

Subsequently, SiO^+ ion beams were injected to a QCM substrate while HMDSO was simultaneously sprayed to the substrate. The duration was 550 min. The injection ion energy was set at 100 eV. After the trial, we found that a film was formed on the QCM substrate. The QCM controller showed that the film thickness was 28 nm. Hereafter, we refer to this film as sample (b).

Sample (a) was analyzed by XPS using an ESCA-3057 X-ray photoelectron spectrometer

equipped with an Al K_α radiation source. The acquired XPS spectra of sample (a) are shown in Fig. 7. The binding energies in the O1s [Fig. 7(a)] and the Si2p [Fig. 7(b)] spectra indicate that the deposited film was silicon oxide [30]. The C1*s* XPS spectrum [Fig. 7(c)] shows that almost no carbon atoms were included in the film.

Subsequently, sample (b) was analyzed by XPS. The XPS spectra of sample (b) are shown in Fig. 8. The binding energies in the O1s [Fig. 8(a)] and the Si2p [Fig. 8(b)] spectra indicate that the deposited film was silicon oxide. The C1*s* XPS spectrum [Fig. 8(c)] shows that sample (b) contained relatively large amount of carbon atoms. The atomic concentration of carbon in the film was 12 atomic%.

Then, the curve fitting of the Si2p peak was carried out. A previous paper reported that five oxidation states (Si, Si^{1+}, Si^{2+}, Si^{3+}, and SiO_2) existed in silicon oxide films [31]. Here, Si^{1+}, Si^{2+} and Si^{3+} represent formal oxidation states [31]. Thus, we decomposed the Si2p peaks [Figs. 7(b) and 8(b)] into five components (Si, Si^{1+}, Si^{2+}, Si^{3+}, and SiO_2) using the least-squares method. The results for samples (a) and (b) are shown in Figs. 9(a) and 9(b), respectively. Fig. 9(a) shows that the Si2p peak can be fitted by the SiO_2 curve alone, suggesting that the resulting film in sample (a) was silicon dioxide (SiO_2). By contrast,

Fig. 9(b) shows that sample (b) contained Si, Si^{1+}, Si^{2+}, Si^{3+}, and SiO_2 peaks. The O concentration of sample (b) could be evaluated using the formula reported in a literature [32] and we found that sample (b) was $SiO_{1.35}$.

Fig. 7(c) shows that sample (a) contained almost no carbon atoms. Although fragment ions produced from HMDSO by the electron impact ionization have been reported [33, 34], fragments produced from HMDSO in the present experimental conditions have not been identified yet. However, we speculate as follows: Firstly, the HMDSO sprayed was adsorbed on the substrate. O^+ ion beams were injected to the substrate, and the kinetic energy of the injected O^+ ions caused the dissociation of HMDSO. On the other hand, the bond energy of Si-C in the HMDSO molecule was much smaller than that of Si-O and C-H bonds, suggesting that Si-C bonds were preferentially broken by the ion beam injection. Therefore, fragments such as SiOSi and CH_3 seem to be produced by the dissociation of HMDSO. We suppose that fragments such as SiOSi were oxidized by injecting O^+ ions and remained on the substrate. Fragments such as CH_3 were also oxidized by O^+ ions through the reaction between C and O atoms [35] and then released from the substrate.

Fig. 6 shows that when HMDSO was supplied to a substrate together with 100 eV SiO^+

ion injections, the film thickness was increased when compared with that obtained by the 100 eV SiO^+ ion injection alone. Therefore, the resulting film was formed by the SiO^+ ions injected to the substrate in addition to HMDSO molecules sprayed to the substrate. Fig. 8(c), however, shows that sample (b) contained a relatively large amount of carbon atoms (12 atomic%). The bond energy of Si-O was much smaller than that of the injecting SiO^+ ion energy (100 eV). Thus, it seems likely that the Si-O bond of the injected ions was broken by the collision between the injected SiO^+ ion and the substrate. The injecting energy of 100 eV was distributed to the constituent atoms. The energies of Si and O atoms were evaluated to be 64 and 36 eV, respectively. In this energy range (64 and 36 eV), the ability of injected Si and O atoms to decompose the HMDSO molecule seems to be low when compared with that of 100 eV O^+ ion beams. Therefore, we suppose that the dissociation of HMDSO molecule by the ion beam injection was insufficient in the SiO^+ ion case and that then the resulting film contained carbon atoms.

We attempted to obtain FTIR spectra of films using the FT/IR-410 (Jasco) instrument. However, the film deposited on the QCM substrate was not suitable for FTIR because infrared radiation did not penetrate the QCM substrate. Therefore, a Si substrate was used instead of the QCM substrate. The experimental parameters were similar to those in the

experiments using the QCM substrate. FTIR spectra of films formed on Si substrates following the injection of (a) 100 eV O^+ and (b) 100 eV SiO^+ ion beams in conjunction with HMDSO were shown in Figs. 10(a) and 10(b), respectively. Figs. 10(a) and 10(b) show that both spectra (a) and (b) have two peaks corresponding to the Si-O-Si stretching mode and the Si-O bending mode, suggesting that the obtained films were silicon oxides. It is noted that peaks around 1500 cm^{-1} in Figs. 10(a) and 10(b) were attributed to water in the ambient air inside the measurement chamber of the FT/IR-410 instrument.

In this study, we found that the 100 eV O^+ or SiO^+ ion beam irradiation in the presence of HMDSO promoted the silicon oxide film formation. In the case of 200 eV ion beam irradiations, the obtained film thickness was thinner than that of the 100 eV case (Figs. 5 and 6). Although the reason for this has not been identified yet, we suppose that the depositing silicon oxide films were sputtered by injecting 200 eV ions. Unfortunately, we could not find any previous papers reporting the sputtering yields of silicon oxides following the O^+ or SiO^+ ion injections. On the other hand, it has been reported that the sputtering of various materials [36] and silicon oxide films [37] by injecting Ar^+ ions increased when the injected ion energy was more than 200 eV. Although the injected ions were not Ar^+ in this study, the finding that the film thickness in the 200 eV case was

thinner than that in the 100 eV case seems to be ascribed to this sputtering effect of injecting ions.

In the present study, we found that silicon dioxide films could be formed when a substrate was irradiated with the 100 eV O^+ ion beam in conjunction with HMDSO. Many studies concerning to silicon oxide depositions using HMDSO have been reported [10-20]. Those studies showed that the atomic concentration of Si, O, and C atoms in the silicon oxides obtained depended on the experimental parameters. Therefore, the authors of those previous studies had to optimize the experimental parameters to reduce the carbon concentration in the film. By contrast, almost no carbon atoms were found included in sample (a) without such a troublesome optimization process.

The deposition rates of silicon oxide films were low in this study. Our ion beam machine was not specifically prepared for film formation experiments but for fundamental investigations of the ion beam effects on various materials. The ion beam intensity was relatively low. In addition, our ion beam machine was not designed for introducing source materials into the process chamber. In this study, we injected only a small amount of HMDSO into the process chamber. For the silicon oxide deposition using the method

presented in this study, it seems to be required to employ other ion beam machines which are capable of introducing both strong ion beam and a large amount of HMDSO into the process chamber.

4. Conclusion

In this study, we conducted an experiment in which HMDSO was sprayed onto a substrate and the substrate was also simultaneously irradiated with O^+ or SiO^+ ions. We found that a film was deposited by the O^+ or SiO^+ ion beam injections in conjunction with HMDSO. We also found that the ion energy at which the film thickness obtained was maximal was 100 eV for both O^+ and SiO^+ cases.

Firstly, 100 eV O^+ ion beams were injected to a substrate while HMDSO was simultaneously sprayed to the substrate. The XPS spectra of the deposited film indicated that the film was silicon dioxide (SiO_2). The C1s spectrum of the film showed that the film contained almost no carbon atoms. Then, 100 eV SiO^+ ion beams were injected to a substrate while HMDSO was simultaneously sprayed to the substrate. The XPS spectra of the deposited film indicated that the film was silicon oxide ($SiO_{1.35}$). The C1*s* spectrum

of the film suggested that the film contained a relatively large amount of carbon atoms (12 atomic%).

In conclusion, we confirmed that the 100 eV O^+ ion beam induced deposition using HMDSO is useful for the silicon dioxide film formation.

Acknowledgments

The authors wish to thank Prof. S. Hamaguchi (Osaka Univ.) for valuable suggestions.

References

[1] K. Miyake, K. Ohashi, H. Takahashi, and T. Minemura, Formation of iron film by ion beam deposition, Surf. Coat. Technol. 65 (1994) 208-213.

[2] H. Ohno, J. A. den Berg, S. Nagai, and D. G. Armour, Growth of carbon thin film by low-energy mass-selected ion beam deposition, Nucl. Instrum. Meth. Phys. Res. B 148 (1999) 673-677.

[3] S. Yoshimura, S. Sugimoto, M. Kiuchi, Low-energy mass-selected ion beam production of fragments produced from hexamethyldisilane for SiC film formation, J. Appl. Phys. 119 (2016) 103302.

[4] D. Leinen, A. Fernandez, J. P. Espinos, T. R. Belderrain, A. R. Gonzalez-Elipe, Ion

beam induced chemical vapor deposition for the preparation of thin film oxides, Thin Solid Films 241 (1994) 198-201.

[5] D. Leinen, A. Fernandez, J. P. Espinos, A. R. Gonzalez-Elipe, Preparation of TiO_2 and Al_2O_3 thin films by ion beam induced chemical vapor deposition, Vacuum 45 (1994) 1043-1045.

[6] J. P. Holgado, M. Perez-Sanchez, F. Yubero, J. P. Espinos, A. R. Gonzalez-Elipe, Corrosion resistant ZrO_2 thin films prepared at room temperature by ion beam induced chemical vapor deposition, Surf. Coat. Technol. 151-152 (2002) 449-453.

[7] S. Yoshimura, S. Sugimoto, T. Takeuchi, K. Murai, M. Kiuchi, Silicon oxide film formation by spraying tetraethyl orthosilicate onto substrate with simultaneous low-energy SiO^+ ion-beam irradiation, AIP Adv. 13 (11) (2023) 115107.

[8] M. F. Ceiler, P. A. Kohl, S. A. Bidstrup, Plasma-enhanced chemical vapor deposition of silicon dioxide deposited at low temperatures, J. Electrochem. Soc. 142 (6) (1995) 2067-2071.

[9] M. A. Lieberman, Principles of plasma discharges and materials processing, A Wiley-Interscience Publication, New York, 1994.

[10] K. Kashiwagi, Y. Yoshida, Y. Murayama, Hybrid films formed from hexamethyldisiloxane and SiO by plasma process, Jpn. J. Apply. Phys. 30 (1991)

1803-1807.

[11] K. Ebihara, T. Fujishima, D. Kojyo, M. Murata, Silicon oxide film preparation by RF plasma-enhanced MOCVD using hexamethyldisiloxane, Plasma Sourc. Sci. Technol. 2 (1993) 14-17.

[12] J. A. Theil, J. G. Brace, R. W. Knoll, Carbon content of silicon oxide films deposited by room temperature plasma enhanced chemical vapor deposition of hexamethyldisiloxane and oxygen, J. Vac. Sci. Technol. A 12 (1994) 1365-1370.

[13] S. E. Alexandrov, N. McSporran, M. L. Hitchman, Remote AP-PECVD of silicon dioxide films from hexamethyldisiloxane (HMDSO), Chem. Vap. Deposition, 111 (2005) 481-490.

[14] A. Pfuch, A. Heft, R. Widl, K. Lang, Characterization of SiO_2 thin films prepared by plasma-activated chemical vapor deposition, Surf. Coat. Technol. 201 (2006) 189-196.

[15] V. Raballand, J. Benedikt, A. von Keudell, Deposition of carbon-free silicon dioxide from pure hexamethyldisiloxane using atmospheric microplasma jet, Appl. Phys. Lett 92 (2008) 091502-1-3.

[16] M. M. Hossain, Q. H. Trinh, D. B. Nguyen, M. S. P. Sudhakaran, Y. S. Mok, Robust hydrophobic coating on glass surface by an atmospheric-pressure plasma jet for

plasma-polymerisation of hexamethyldisiloxane conjugated with (3-aminopropyl) triethoxysilane, Surf. Eng. 35 (2019) 466-475.

[17] S. Saloum, S. A. Shaker, M. N. Alkafri, A. Obaid, R. Hussin, Effect of surface modification on the properties of plasma-polymerized hexamethyldisiloxane thin films, Surf. Interface Anal. 51 (2019) 754-762.

[18] M. A. Gilliam, S. A. Farhat, G. E. Garner, B. P. Stubbs, B. B. Peterson, Characterization of the deposition behavior and changes in bonding structures of hexamethyldisiloxane and decamethylcyclopentasiloxane atmospheric plasma-deposited films, Plasma Proess Polym. 16 (2019) e1900024.

[19] E. Kermaneci, F. Mitschker, J. Benedikt, D. Eremin, P. Awakowicz, R. P. Brinkmann, A numerical analysis of a microwave induced coaxial surface wave discharge fed with a mixture of oxygen and hexamethyldisiloxane for the purpose of deposition, Plasma Sources Sci. Technol. 28 (2019) 115003.

[20] T. Saito, R. Mitsuya, Y. Ito, T. Higuchi, T. Aita, Microstructured SiO_x thin films deposited from hexamethyldisilazane and hexamethyldisiloxane using atmospheric pressure thermal microplasma jet, Thin Solid Films 669 (2019) 321-328.

[21] S. Yoshimura, S. Sugimoto, K. Murai, M. Kiuchi, Low-energy mass-selected ion beam production of fragments produced from hexamethyldisiloxane for the

formation of slicon oxide film, Surf. Coat. Technol. 313 (2017) 402-406.

[22] T. Matsutani, T. Asanuma, C. Liu, M. Kiuchi, T. Takeuchi, Deposition of SiO_2 films by low-energy ion-beam induced chemical vapor deposition using hexamethyldisiloxane, Surf. Coat. Technol. 177-178 (2004) 365-368.

[23] S. Yoshimura, S. Sugimoto, T. Takeuchi, K. Murai, M. Kiuchi, Effects of injected ion energy on silicon carbide film formation by low energy $SiCH_3^+$ beam irradiation, Thin Solid Films 685 (2019) 408-413.

[24] S. Yoshimura, S. Sugimoto, T. Takeuchi, K. Murai, M. Kiuchi, Low-energy Ar^+ and N^+ ion beam induced chemical vapor deposition using hexamethyldisilazane for the formation of nitrogen containing SiC and carbon containing SiN films, PLOS ONE 16(10) (2021) e0259216.

[25] S. Yoshimura, K. Ikuse, M. Kiuchi, Y. Nishimoto, M. Yasuda, A. Baba, S. Hamaguchi, Dependence of catalytic properties of indium implanted SiO_2 thin films on the film-substrate temperature during indium ion implantation, Nucl. Instrum. Methods Phys. Res. B 315 (2013) 222-226.

[26] S. Yoshimura, K. Hine, M. Kiuchi, J. Hashimoto, M. Terauchi, Y. Honda, M. Nishitani, S. Hamaguchi, Experimental evaluation of CaO, SrO, and BaO sputtering yields by Ne^+ or Xe^+ ions, J. Phys. D: Appl. Phys. 44 (2011) 255203.

[27] S. Yoshimura, Y. Tsukazaki, M. Kiuchi, S. Sugimoto, S. Hamaguchi, Sputtering yields and surface modification of poly(methyl methacrylate) (PMMA) by low-energy Ar^+/CF_3^+ ion bombardment with vacuum ultraviolet (VUV) photon irradiation, J. Phys. D: Appl. Phys. 45 (2012) 505201.

[28] K. Hine, S. Yoshimura, K. Ikuse, M. Kiuchi, J. Hashimoto, M. Terauchi, M. Nishitani, S. Hamaguchi, Experimental evaluation of MgO sputtering yields by monochromatic Ne, Kr, or Xe ion beams, Thin Solid Films 517 (2008) 835-840.

[29] S. Yoshimura, A. Toh, S. Sugimoto, M. Kiuchi, S. Hamaguchi, Fragment ions od dimethylsilane produced from hot tungsten wires, Jpn. J. Appl. Phys. 45 (2006) 8204-8207.

[30] R. Bertoncello, A. Glisenti, G. Granozzi, G. Battaglin, F. Caccavale E. Cattaruzza, P. Mazzoldi, Chemical interactions in titanium- and tungsten-implanted fused silica, J. Non-Crystall. Solids 162 (1993) 205-216.

[31] G. Hollinger, F. J. Himpsel, Probing the transition layer at the SiO2-Si interface using core level photoemission, Appl. Phys. Lett. 44 (1984) 93-95.

[32] J. R. Shallenberger, Determination of chemistry and microstructure in SiO_x films by x-ray photoelectron spectroscopy, J. Vac. Sci. Technol. A 14 (1996) 693-698.

[33] S. Tobita, S. Tajima, F. Okada, S. Mori, E. Tabei, M. Umemura, Metastable ion study

of organosilicon compounds, Org. Mass Spectrom. 25 (1990) 39-43.

[34] S. Yoshimura, S. Sugimoto, T. Takeuchi, M. Kiuchi, Production of low-energy fragment-ion beams from hexamethyldisiloxane and the irradiation of SiO^+ ion beam to substrates with supplemental oxygen gas for SiO_2 film formation, Nucl. Instrum. Methods Phys. Res. B 479 (2020) 13-17.

[35] E. Vietzke, T. Tanabe, V. Philipps, M. Erdweg, K. Flaskamp, The reaction of energetic O_2^+, thermal O_2, and thermal O_2/Ar^+ on graphite and the use of graphite for oxygen collector probes, J. Nucl. Mat. 145-147 (1987) 425-428.

[36] Y. Yamamura, H. Tawara, Energy dependence of ion-induced sputtering yields from monatomic solids at normal incidence, Atom. Data Nucl. Data Tables 62 (1996) 149-253.

[37] D. C. Gray, I. Tepermeister, H. H. Sawin, Phenomenological modeling of ion-enhanced surface kinetics in fluorine-based plasma etching, J. Vac. Sci. Technol. B 11 (4) (1993) 1243-1257.

Figure captions

Fig. 1

A schematic drawing of the process chamber in our ion beam experiments.

Fig. 2

Mass spectra in (a) O^+ and (b) SiO^+ ion beam experiments.

Fig. 3

Energy spectra of O^+ ion beams in (a) 50, (b) 100, and (c) 200 eV cases.

Fig. 4

Energy spectra of SiO^+ ion beams in (a) 50, (b) 100, and (c) 200 eV cases.

Fig. 5

The dependence of film thickness on injecting O^+ ion energy levels. The films were obtained following the injection of O^+ ion beams to a quartz crystal microbalance substrate in conjunction with hexamethyldisiloxane.

Fig. 6

closed circles: The dependence of film thickness on injecting SiO^+ ion energy levels. The

films were obtained by the injection of SiO^+ ion beams to a quartz crystal microbalance substrate in conjunction with hexamethyldisiloxane.

closed triangles: The dependence of film thickness on injecting SiO^+ ion energy levels. The films were obtained by the injection of SiO^+ ion beams alone.

Fig. 7

(a) O1s, (b) Si2p and (c) C1s X-ray photoelectron spectroscopy spectra of a film obtained by injecting 100 eV O^+ ion beams to a quartz crystal microbalance substrate in conjunction with hexamethyldisiloxane.

Fig. 8

(a) O1s, (b) Si2p, and (c) C1s X-ray photoelectron spectroscopy spectra of a film obtained by injecting 100 eV SiO^+ ion beams to a quartz crystal microbalance substrate in conjunction with hexamethyldisiloxane.

Fig. 9

The curve fitting of the Si2p peak using the least-squares fitting method. (a) The Si2p spectrum of a film, obtained following the injection of 100 eV O^+ ion beams to a quartz

crystal microbalance substrate in conjunction with hexamethyldisiloxane, is shown by closed circles. The solid line is the fitted curve (SiO_2) to the Si2p peak. (b) The Si2p spectrum of a film, obtained following the injection of 100 eV SiO^+ ion beams to a quartz crystal microbalance substrate in conjunction with hexamethyldisiloxane, is shown by closed circles. The dashed line is the fitted curve to the Si2p peak. Five components (Si, Si^{1+}, Si^{2+}, Si^{3+}, and SiO_2) decomposed from the Si2p peak are shown by solid lines.

Fig. 10

Fourier transform infrared spectra of films formed on Si substrates following the injection of (a) 100 eV O^+ and (b) 100 eV SiO^+ ion beams in conjunction with hexamethyldisiloxane.

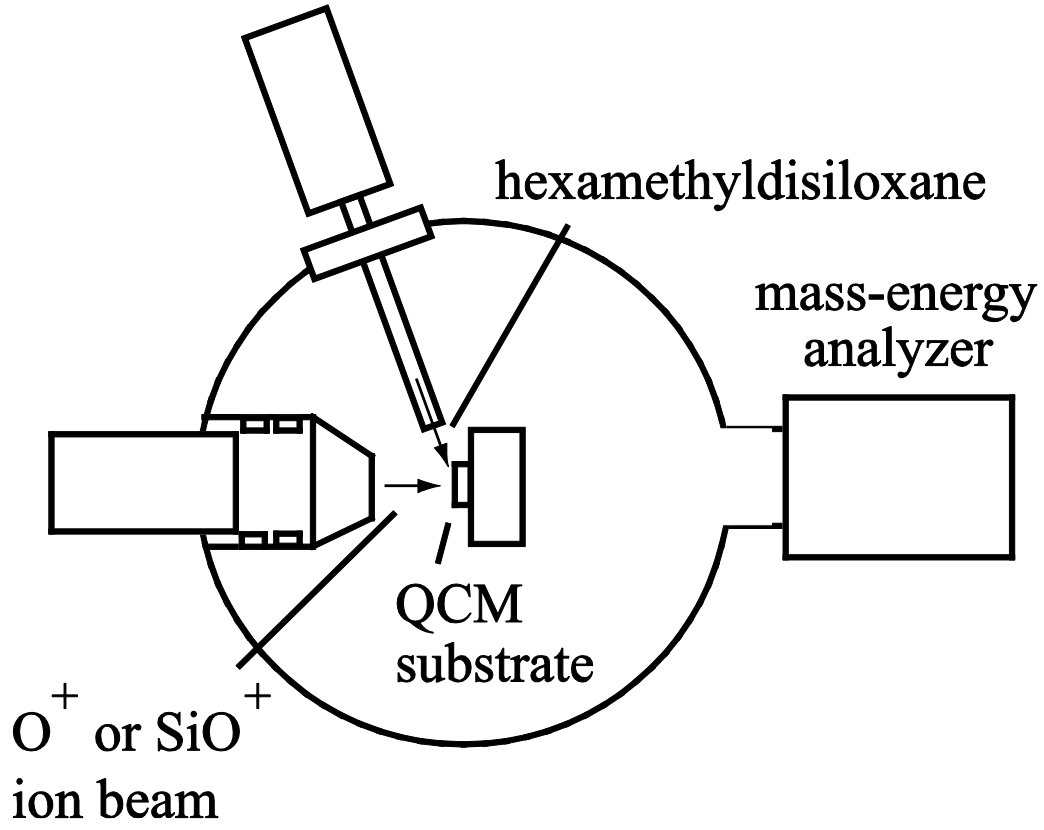
hexamethyldisiloxane
mass-energy
analyzer
QCM
substrate
O+ or SiO+
ion beam

Fig. 1

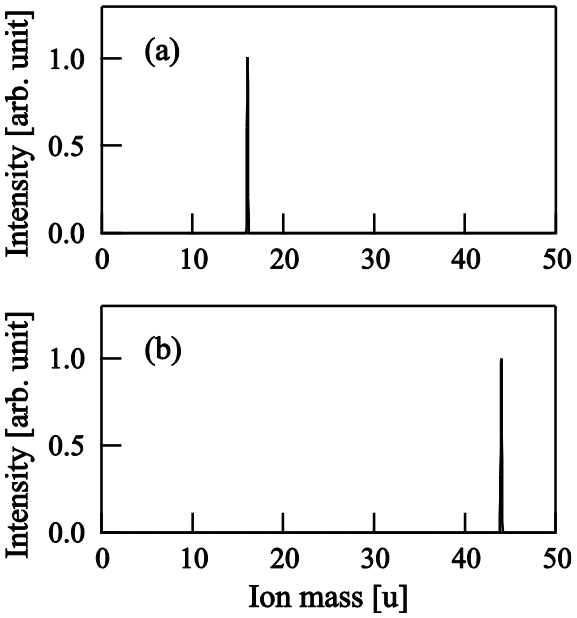
(a)
(b)
Intensity [arb. unit]
Intensity [arb. unit]
1.0
0.5
0.0
1.0
0.5
0.0
0
10
20
30
40
50
0
10
20
30
40
50
Ion mass [u]

Fig. 2

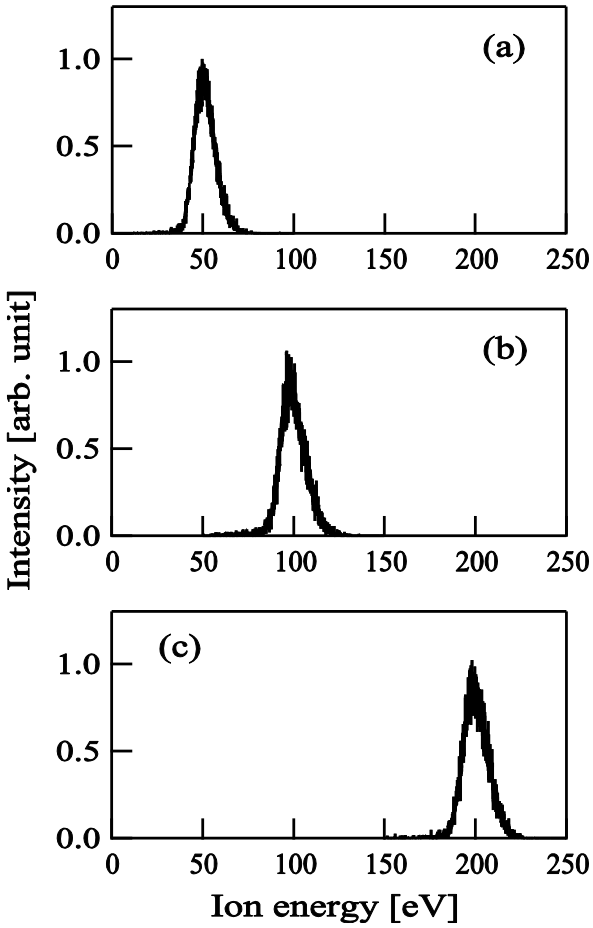
(a)
(b)
(c)
1.0
0.5
0.0
0
50
100
150
200
250
Intensity [arb. unit]
Ion energy [eV]

Fig. 3

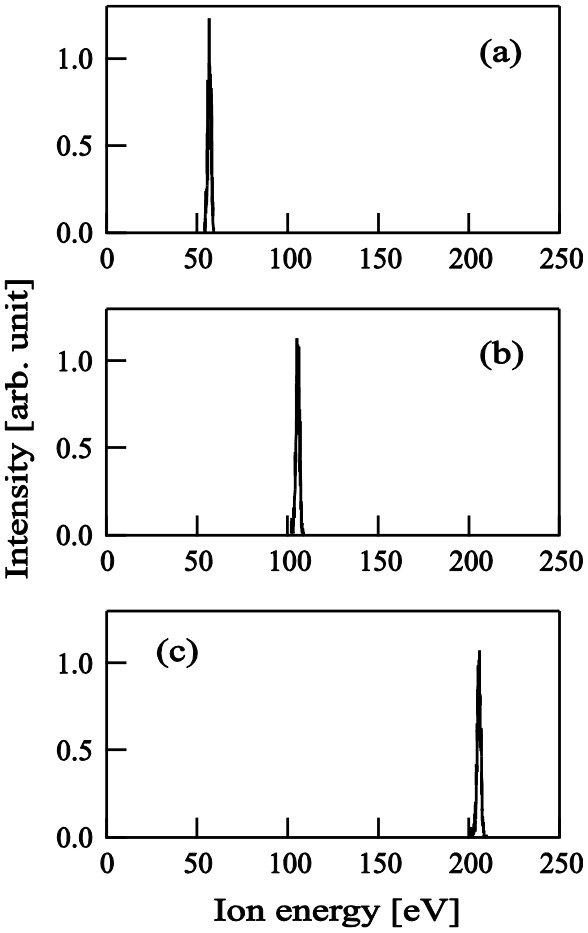
(a)
(b)
(c)
1.0
0.5
0.0
0
50
100
150
200
250
Intensity [arb. unit]
Ion energy [eV]

Fig. 4

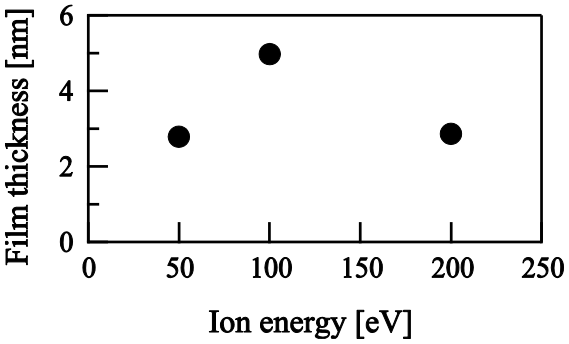

Fig. 5

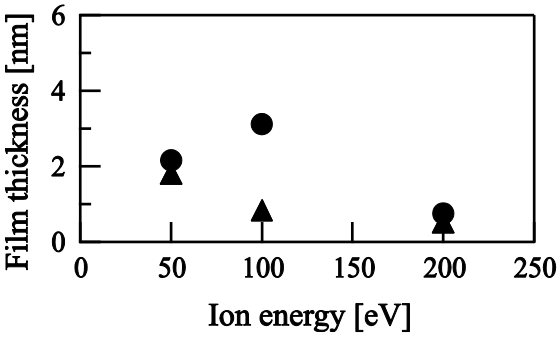

Fig. 6

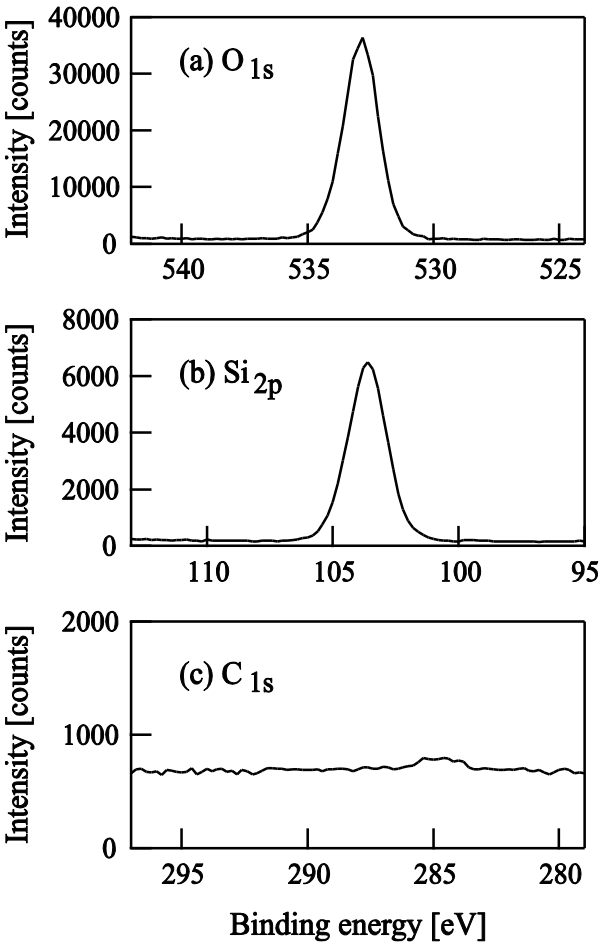
(a) O 1s
(b) Si 2p
(c) C 1s
Intensity [counts]
Binding energy [eV]
40000
30000
20000
10000
0
540
535
530
525
8000
6000
4000
2000
110
105
100
95
1000
295
290
285
280

Fig. 7

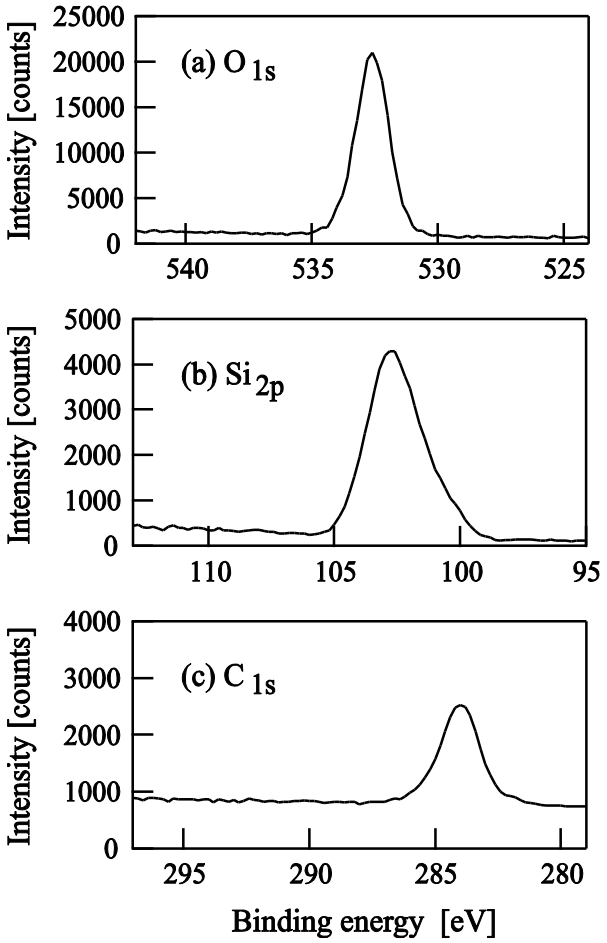
Intensity [counts]
25000
20000
15000
10000
5000
0
(a) O 1s
540
535
530
525
Intensity [counts]
5000
4000
3000
2000
1000
0
(b) Si 2p
110
105
100
95
Intensity [counts]
4000
3000
2000
1000
0
(c) C 1s
295
290
285
280
Binding energy [eV]

Fig. 8

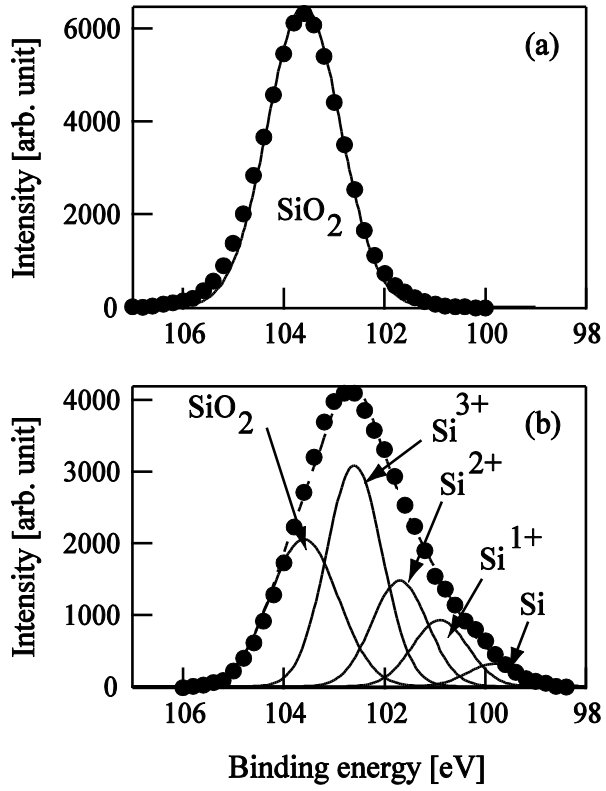
Intensity [arb. unit]
6000
4000
2000
0
(a)
SiO2
106
104
102
100
98
Intensity [arb. unit]
4000
3000
2000
1000
0
SiO2
Si3+
Si2+
Si1+
Si
(b)
106
104
102
100
98
Binding energy [eV]

Fig. 9

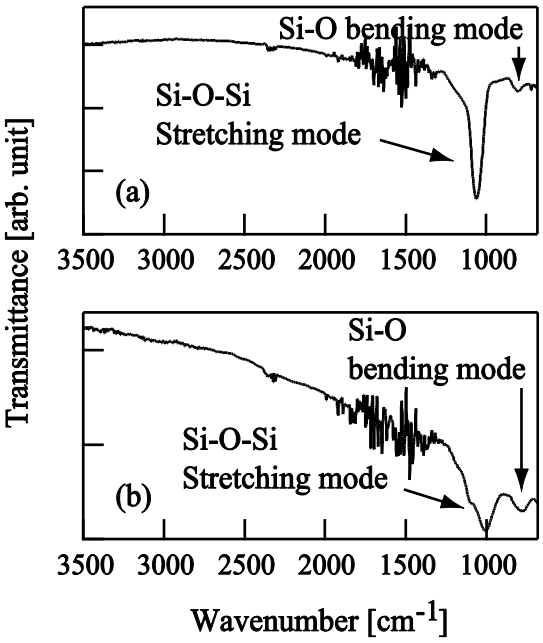
Si-O bending mode
Si-O-Si
Stretching mode
(a)
3500 3000 2500 2000 1500 1000
Si-O
bending mode
Si-O-Si
Stretching mode
(b)
3500 3000 2500 2000 1500 1000
Transmittance [arb. unit]
Wavenumber [cm-1]

Fig. 10